Proceedings of the 2008 IEEE/ASME
International Conference on Advanced Intelligent Mechatronics
July 2 - 5, 2008, Xi'an, China

Design and Experiments on a New Wheel-Based Cable Climbing Robot*

Fengyu Xu
School of Mechanical Engineering
Southeast University
Nanjing, 210096, China

Xingsong Wang
School of Mechanical Engineering
Southeast University
Nanjing, 210096, China
xswang@seu.edu.cn

***Abstract*—This paper proposes an ameliorated wheel-based cable inspection robot, which is able to climb up a vertical cylindrical cable on the cable-stayed bridge. The newly-designed robot in this paper is composed of two equally spaced modules, which are joined by connecting bars to form a closed hexagonal body to clasp on the cable. Another amelioration is the newly-designed electric circuit, which is employed to limit the descending speed of the robot during its sliding down along the cable. For the safe landing in case of electricity broken-down, a gas damper with a slider-crank mechanism is introduced to exhaust the energy generated by the gravity when the robot is slipping down. For the present design, with payloads below 3.5kg, the robot can climb up a cable with diameters varying from 65mm to 205mm. The landing system is tested experimentally and a simplified mathematical model is analyzed. Several climbing experiments performed on real cables show the capability of the proposed robot.**

Index Terms – Cable-stayed bridge, climbing robot, slider-crank mechanism, gas damper.

I. INTRODUCTION

Climbing robots have various applications in industry and dangerous situations: inspection of high chimneys, inspection of vertical and inclined pipes in nuclear power plants and inspection of wiring on high voltage power transmission towers, all these are typical examples of its applications [1].Moreover, there are some new and other important tasks for these robots, for instance, examining cables on a cable-stayed bridge.

Cable is one of the most important stress components of the cable-stayed bridges. In the United States, several cable-stayed bridges have shown signs of cable damages mostly induced by susceptibility of stay cables to wind-induced vibrations and corrosion [2]. It has caused public concerns and initiated a series of inspection and security monitoring programs. The cables must be examined periodically to ensure the reliability of the bridge. For a long time, the inspection was conducted artificially, which is inefficient and dangerous. Under these circumstances, this paper proposed a new wheel-based cable climbing robot for the cable inspection.

Climbing robots belong to a specialized field of mobile robots. The main feature is the mobility against gravity of the body. An important aspect to consider in the design of such robots is that they need to be lightweight and powerful enough to move up to support their own weight [3]. Therefore, the designer should consider not only the locomotion method, as in conventional mobile robots, but also the techniques sticking to the cable. There are already several forms of adhesion methods:

(1) Magnetic mechanisms for climbing on ferrous surfaces via electromagnets or permanent magnets [4].

(2) Vacuum suction technologies for sticking the robot on the walls [5] [6].

(3) Grippers or armed mechanisms that attach to the structure such as beams, columns, pipes, and tubes [7].

According to the modes of adhesion, climbing robots can be classified into three main groups:

(1) Wheel-driven machines climb vertical planes by combining wheels for translation, and by magnets or vacuum suction for surface attachment [8];

(2) Legged climbing robots [9] consist usually of four or six legs, each of which with magnets or a vacuum pump for attachment, but the maneuverability of these mechanisms is limited;

(3)Locomotion based on arms with grippers or other devices that provide the robot with skillful mobility [10] [11] [12].

The climbing robot proposed in this paper utilized springs to provide friction forces to support the whole robotic systems. With the driving wheel actuated by a powerful DC motor, the robot can climb on a cable inclined at any angles, including a vertical one.

II. STRUCTURE AND STATICS OF THE ROBOT

The principle of the climbing robot is shown in Fig.1. The maximal static friction force to hold the mechanism is denoted by F .

For mechanism in Fig.1, we have:

$F = \mu N \geq G$

μ -static friction coefficient,

N -clasping force,

G -the gravity of the climbing mechanism and the load.

In order to less the clasping force, the friction coefficient of the wheel coating material to the cable should be as large as possible. The required driving force to climb is denoted as Q, and it is obvious that $Q \geq F$

$Q = G + \mu_1 N$

* This work was supported by the National 863 plan (No.2006AA04Z234) and New Century Excellent Talent Plan of MOE of China (No. NCET-04-0479).

μ_1 - coefficient of rolling friction.

So the required power of DC motor P is:

$P = QV/\eta = (G + \mu_1 N)V/\eta$

V - the climbing velocity of the mechanism,

η - driving efficiency.

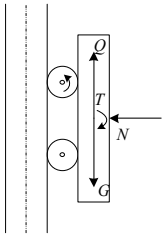

Fig.1 Principle of Climbing.

Unlike our previously designed climbing robot which was a trisected robot [14], there are several improvements introduced here.

The first improvement is that the climbing robot proposed here (shown in Fig.2), is composed of two equally spaced modules facing each other. Only one of the two modules is powered and the other is passive. Each module possesses two wheel limbs at the two ends. Only the upper wheel of the powered module is actuated with a DC motor. The passive module is applied to provide the supporting force and improve the system stability.

The two modules are joined by eight connected bars to form a whole closed hexagonal body to clasp the cable. By changing the joined holes of the connecting bars, the robot can climb cables with varied diameters. All the wheels (including the driving wheel) were machined in V-shape with open angle $\phi = 150°$ to increase the contacting area. This will also reduce the abrasion, prevent the driving wheel from deflecting off the cable, and avoid getting stuck.

As shown in Fig.3, the wheel limbs of the passive module are connected with an extension spring to provide the robot with enough clasping force. The limbs hinged with the body of the passive module also enable the robot climbing over small obstacles by the elongating of the springs. In order to reduce the drag force and to ensure only one wheel crawl over the obstacle at one time, the passive wheel was offset "d" from the driving wheel [14].

For the driving module, as shown in Fig.4, through a bevel gear reducer, the motor drives the wheel fixed on the body of the powered module via a magnetic clutch. In case of power shortage or electrical failure, to guarantee the robot to slip down safely, there is also a safety landing mechanism attached to the driving wheel through a one-way clutch. This is the second improvement. The principle of the safety landing mechanism will be discussed in detail in section 4.

When the robot climbs up, the magnetic clutch is locked to the driving shaft and in this way the driving power acts on the driving wheel directly. Meantime, the one-way clutch is free and the landing mechanism does not work.

An encoder is applied to measure the distance between the robot and ground. And there is moustache sensor to detect the top end of the cable. When it arrives at the top end, the driving motor will be powered off and the robot will slip downward by its gravity. At this time the safety landing mechanism will work to ensure the safe landing without consuming any energy.

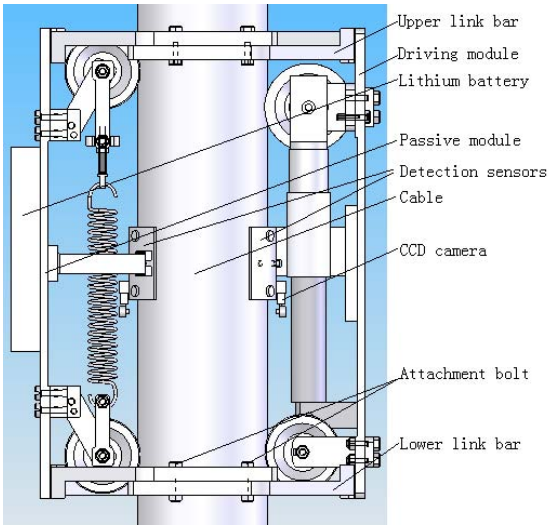

Fig. 2 Structure of the Climbing Robot

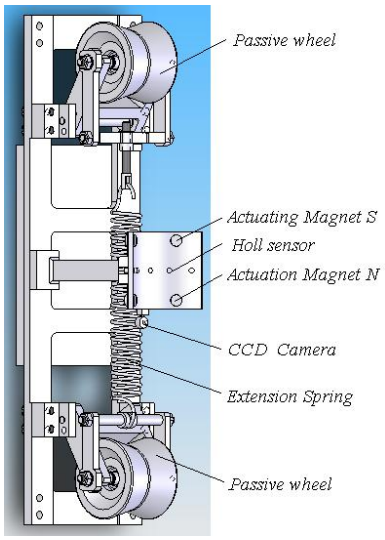

Fig 3 Passive Module of the Robot.

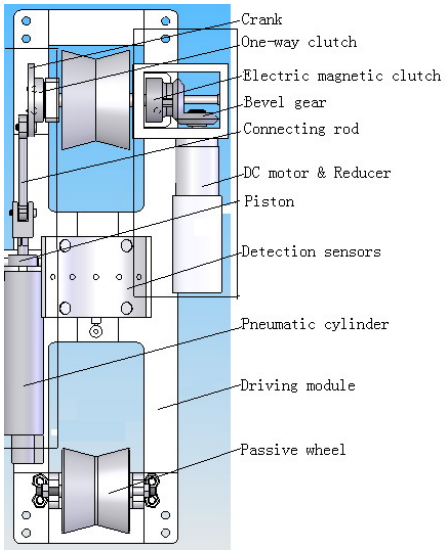

Fig.4 Structure of the Driving Vehicle.

III. Principle of Descending Speed Restriction

When the motor is powered off, the electronic circuit changes the motor to an electric generator, where the driving wheel drives the armature running wheel the robot slips down along the cable. The armature cuts the magnetic flux and the back torque forms. Since the kinetic energy is changed to electrical energy, different slipping velocities can be reached by adjusting the load resistance. The schematic diagram of the DC motor established according to above statements is given in Fig.5.

The equations describing the motor behaviors are:

$$V_R = E_a - R_a i_a + L_a(di_a/dt) \quad (1\text{-a})$$

$$E_a = K_e \phi n \quad (1\text{-b})$$

$$T_m = K_t \phi i_a \quad (1\text{-c})$$

$$i_a = \frac{E_a}{R + R_a} \quad (1\text{-d})$$

$V_R(V)$ is the voltage on variable resistance;

$R_a(\Omega)$ is the resistance of the armature coil;

$L_a(H)$ is the inductance of the armature coil;

R is the value of variable resistance;

$i_a(A)$ is the current of the armature;

$T_m(Nm)$ is the back torque generated by the motor;

ϕ is the magnetic flux;

$K_e, K_t(Vs/rad)$ is the torque constant of the motor;

$E_a(V)$ is the induced electromotive force;

$n(r/m)$ is the rotational speed of the motor.

The driving moment acting on the robot is

$$\tau_2 = r_1(Mg\sin\theta - F_f) - \tau_3 \quad (2)$$

F_f is the total friction force between the wheels and the cable;

τ_3 is the friction moment of the motor;

M is the mass of the robot and the payload;

θ is the tilt angle of the cable.

When the robot is slipping at a constant speed, we have

$$T_m = \tau_2$$

From the equations (1) (2), the descending speed of the robot can be deduced as,

$$v = \frac{(r_1(Mg\sin\theta - F_f) - \tau_3)(R + R_a)}{iK_t\phi K_e\phi} \cdot \frac{2\pi r_1}{60i} \quad (3)$$

Where, i is the ratio of the speed reducer.

By selecting the value of the resistance (R), the speed of the robot can be adjusted and confined with varied loads on different cables.

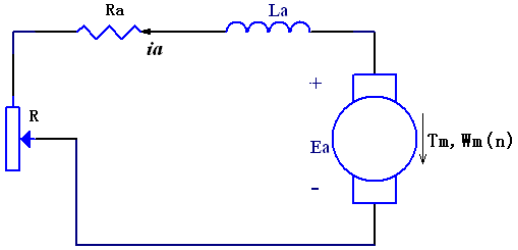

Fig.5 Schematic Diagram of the DC Motor Serving as a Generator

IV. Analysis of the Safety Landing Mechanism

In this section, the second big improvement of the landing speed constraint mechanism is introduced. In order to make the robot land in a controllable velocity (the value is not too large) in case of power shortage or electrical failure, the newly-designed robot have a falling speed control mechanism consisting of a pneumatic cylinder and a slider-crank mechanism whose crank is fixed with the driving shaft through the one-way clutch (as shown in Fig.4). While the robot is slipping down, the rotation motion of the driving wheel is transmitted to the piston's reciprocating motion in the pneumatic cylinder. The gas in the cylinder inhaled or ejected alternately from the hole forms a gas damper to consume the kinetic energy of the robot. The size of the hole can be adjusted to obtain different damper ratios so as to control the landing speed of the robot.

The principle of the landing mechanism is shown in Fig.6. A slider-crank mechanism is a single–looped mechanism, which has a constrained condition as follows:

$$\beta = \arcsin(r_2/l \cdot \sin\alpha) \quad (4)$$

The rotary inertia of the connecting rod is very small, so the connecting rod can be considered as a two-force member neglecting its reciprocating and rotating,

$$Fe = \frac{A(p_0 - p) - m_2\alpha}{\cos\beta}$$

For the crank, the angular velocity and the acceleration are:

$$\begin{cases} w = d\alpha/dt \\ \varepsilon = J^{-1}(\tau - Fe \cdot r_2 \cdot \sin(\alpha + \beta)) \end{cases} \quad (5)$$

α is the acceleration of the piston.

The displacement of the piston is:

$$\begin{cases} x = B + L + r_2 - r_2(\cos\alpha + \lambda/4\cos 2\alpha - \lambda/4) \\ \lambda = r_2/l \end{cases} \quad (6)$$

The speed and acceleration of piston are as follows:

$$\begin{cases} V = \dfrac{dx}{dt} = r_2\dfrac{d\alpha}{dt}(\sin\alpha + \dfrac{\lambda}{2}\sin 2\alpha) \\ \alpha = \dfrac{dV}{dt} = r_2 w^2(\cos\alpha + \lambda\sin 2\alpha) \end{cases} \quad (7)$$

When slipping down from the cables, the robot accelerates at the beginning, and fluctuates after the velocity achieves a fixed value. So the robot is in quasi-uniform motion, the approximate torque acting on the crankshaft is:

$$\tau_2 = r_2 Mg$$

The physical process involving in the emission and suction of gas is very complex. To simplify the analysis, some assumptions are made: (1) the gas flows adiabatically in the cylinder and it is isentropic at the release point; (2) the model of flow is considered as one-dimension.

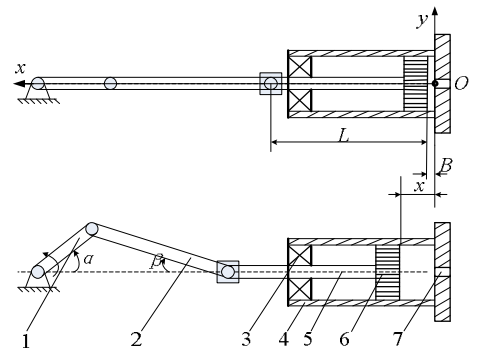

(a)

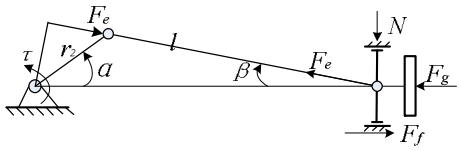

(b)

Fig.6 Safety Landing Mechanism
1crank; 2connecting rod; 3linear bearing; 4 pneumatic cylinder; 5 piston connecting rod; 6 piston; 7 nozzle.

The value of the release rate in the hole depends on whether gas flow is sonic or subsonic. This will be decided by the critical pressure ratio [13]:

$$CPR = (\frac{2}{1+k})^{\frac{k}{k-1}} = 0.528$$

When $CPR \le 0.528$, the gas release in the hole is a sonic flow. The release rate passing the orifice is described by the following equation:

$$Q = \mu A P_1 \sqrt{k \frac{M}{ZRT} (\frac{2}{1+k})^{\frac{k+1}{k-1}}} \tag{8}$$

When $CPR \succ 0.528$, the gas release is subsonic, and the release rate is:

$$Q = \mu A P_1 \sqrt{\frac{M}{ZRT} \cdot \frac{2k}{k-1} \cdot [(\frac{p_0}{p_1})^{\frac{2}{k}} - (\frac{p_0}{p_1})^{\frac{k+1}{k}}]} \tag{9}$$

The specific volume is:

$$\nu = 1/\rho = m/V$$

So the volume flow is:

$$\Delta C = \begin{cases} \mu A_{or} P_1 \nu \sqrt{k \cdot \frac{M}{ZRT} \cdot (\frac{2}{k+1})^{\frac{k+1}{k-1}}} \\ \mu A_{or} P_1 \nu \sqrt{\frac{M}{ZRT} \cdot \frac{2k}{k-1} \cdot [(\frac{p_0}{p_1})^{\frac{2}{k}} - (\frac{p_0}{p_1})^{\frac{k+1}{k}}]} \end{cases} \tag{10}$$

Where A_{or} is the area of hole(m2), C is the empirical discharge coefficient(for subsonic gas of Reynolds number larger than 30,000, C=0.61; for other situations C=1, Q is mass flux (kg m-2s-1)), Q is release rate(kg s-1), K is heat capacity ratio, M is molecular weight(kg/k mol), P_1 is pressure of the upstream(Pa), R is the constant of gas(Pa m3 Mol-1 K-1), T is the temperature of gas (K), ρ is density of gas(kg m-3), J is inertia of the crank.

The pressure in the cylinder is influenced by two factors: (1) the variety of the cylinder's volume caused by the movement of the piston; (2) the gas flow through the hole caused by the pressure difference inside and outside of the cylinder.

$$P_t = P(\frac{V_0}{V_0 + \Delta V})^K \pm P(\frac{\Delta C}{V_0 + \Delta V})^K \tag{11}$$

P_t is the instantaneous pressure after the movement of the piston and the gas flowed; P is the instantaneous pressure; V_0 is the original volume; the value of ΔV, the variety of the volume caused by the piston, is positive when the volume is increasing, otherwise ΔV is negative; ΔC is the volume flow mentioned above.

The Quasi-steady-state (QSS) simulation methodology is used to simulate the landing mechanism. The whole concept is to replace the transient dynamic state by its QSS equilibrium state. Divide the whole process into many small time segments, denoted as Δt, each of which is a simulation step. One can regard this process as a steady-state when Δt is small enough. The change of pressure and the movement of the piston occur simultaneously. The air input of the cylinder is calculated according to the steady discharge. This is called quasi-steady-state simulation methodology which is applied widely in engineering. With the method, according to the state at the beginning of Δt, one can obtain the piston's motion state and the pressure in the cylinder at the end of Δt, which can be the parameters used in the next Δt. The smaller Δt is divided, the more accurate precision is obtained. By adjusting Δt, the accuracy of simulation will increase. This is called varying-step simulation.

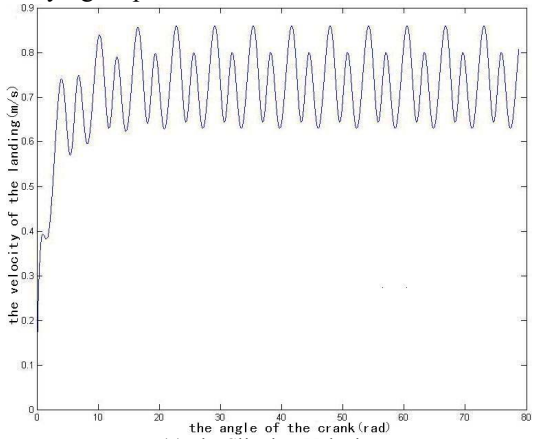

(a) the Slipping Velocity

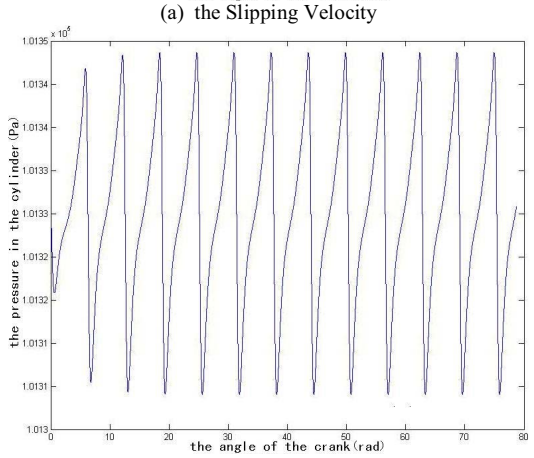

(b) the pressure in the cylinder

Fig.7 Landing Velocity and the Cylinder Pressure.

Fig.7 is simulation curve of the landing velocity and the pressure in the cylinder when the robot is slipping down a vertical cable of 19m high. The abscissa is the angle of the crank. The diameter of the tested cable is 139 mm, the diameter of the hole in the gas cylinder is 3mm. When reached 0.75m/s, the velocity began to fluctuate at the velocity of 0.75m/s.

V. EXPERIMENTS

There are three cables and a wind tunnel in the experiment, as shown in Fig.8. Varied tests of movement were performed on horizontal, inclined and vertical cables. The robot with 3.5 kg payload was first tested on a vertical cable (5 meters long and used on Sutong Bridge) with 3-millimeter obstacle placed according to actual expanded surface of the polyethylene sleeves on the cable surface. Later, it was tested on rough surface of a 75°-inclined cable, similar to the one on Sutong Bridge, to prove the stability of wheel on the cable. The third test was performed in the wind tunnel. All the tests performed gave good results, and in no case did the wheels uncontrollably slip along the cable. The robot can stably climb along the rough vertical cable surface in 8 class wind.

When the robot reaches the top of the cable, the power was cut off, and then it returned to the ground safely with the speed restriction. The speed recorded in the laboratory is shown in Fig. 9: (a) and (c) show the curve of the robot's landing velocity, by the action of both back electromotive force and the gas restriction, down from the 30° -inclined cable and a vertical one respectively; (b) and (d) show the curve of the robot's landing velocity, by the gas restriction only, down from the 30° -inclined cable and a vertical one respectively.

Fig.10 shows the spot tests on a cable-stayed bridge in WuHan, China. The object is the sixth cable, the diameter of which is 105mm, the length 130m, the angle 67° . The results proved the robot could be used to inspect the bridge.

(a)The test in wind tunnel

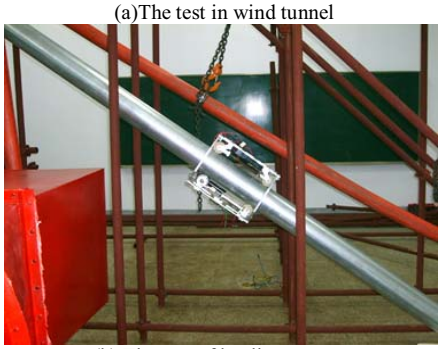

(b) The test of landing system

Fig.8 The Experimental Environment.

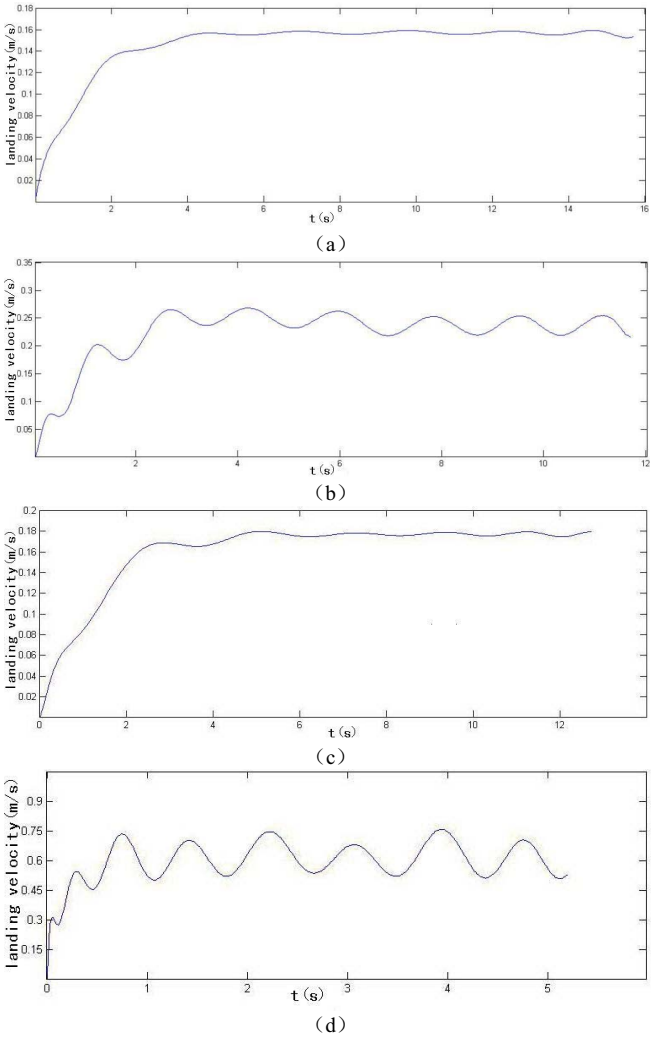

Fig.9 Landing Velocity of the Robot

Fig.10 Field test of the Mechanism

From the experiments we can conclude:

(1)The robot can bear 3.5 kg payload to pass across a small obstacle (about 3mm) and climb along the cable with diameters varying from 65mm to 205mm, which meets the demands of cable detecting tasks.

(2)By both back electromotive force and the gas restriction, the robot can land at a proper and uniform speed, which can be changed by adjusting the resistance.

(3)In case of the electricity broken-down, the robot can return to the ground by gas damper in fluctuated velocity (0.52 m/s-0.68m/s), which can ensure the safety of landing though isn't suitable for inspection.

VI. Conclusion and Future Works

In this paper, the authors designed an innovated wheel-based cable climbing robot whose advantages are the small physical volume, simple structure and light weight. The experiment results indicate that the robot can climb up cable stably. When the robot lands at a low speed (below 0.25m/s), the effect of the gas damper isn't obvious, and the fluctuation of the velocity can be neglected. Therefore, the two landing methods can be used simultaneously to increase the reliability and meet the demands of energy-saving recovery and return in case of accident.

Further work in vortex-induced cable vibration of cable and study on the leakage inspecting method are needed to consummate perfect the whole system.

Acknowledgement

The authors would like to express our special thanks to the valuable advice given by professor Xiaoyuan He.

This work was supported by the 863 Plan under the grant number:2006AA04Z234, and New Century Excellent Talent plan of MOE of China, 2004. (No. NCET-04-0479).

References

[1] D.Bevly, Steven D. and C. Mavroidis, "A Simplified Cartesian Computed Torque Controller for Highly Geared Systems and Its Application to an Experimental Climbing Robot," Journal of Dynamic Systems, Measurement and Control, Trans. ASME, 122(1), 2000, pp. 27-32.

[2] Mehrabi, Armin B., Telang, Niket M., Ghara, Hossein, Fossier, Paul, "Health monitoring of cable-stayed bridges - A case study, Proceedings of the 2004 Structures Congress - Building on the Past: Securing the Future", May 22-26, 2004, Nashville, TN, United State, pp. 59-66

[3] Zaidi Mohd,Tan Beng Soon, A.B.Abdullah, "Development of a Low –Cost Modular Pole Climbing Robot," TENCON 2000 Proceedings, 2000, pp.196-200

[4] Wang Yan, Liu Shuliang, Xu Dianguo etc., "Development and application of Wall-Climbing Robots," Proc. of the 1999 IEEE International Conference on Robotics and Automation, Detrout, Michigan, 1999,pp. 1207-1212,

[5] Briones.L, Bustamante.P, Serna.M. A, "Wall-climbing robot for inspection in nuclear power plants," Proc. of the 1994 IEEE International Conference on Robotics and Automation, 1994, pp.1409-1414.

[6] G.La Rosa, M.Messina, G.Muscato, "A low-cost lightweight climbing robot for the inspection of vertical surfaces," Mechatronics 12(1), 2002, pp.71-96

[7] T.White, N.Hewer, N.Luk, "The design and operational performance of a climbing robot used for weld inspection in hazardous environments,"Proc.1998 IEEE International Conference on Control Applications, Trieste, Italy, 1998, pp.451-455.

[8] S.Weimin, G.Jason, S.Yanjun, "Permanent Magnetic System Design for the Wall-climbing Robot," Proc. of the IEEE International
Conference on Mechatronics and Automation, Niagara Falls, Canada, 2005, pp.2078-2083.

[9] Bing L.Luk, David S.Cooke, Stuart Galt, "Intelligent legged climbing service robot for remote maintenance applications in hazardous environments," Robotics and Autonomous Systems, 53(2005), 2005, pp.142-152

[10] C.Balaguer, J.Pastor, A. Gimenez, V. pardon, and M. Abderrahim, "ROMA: Multifunctional autonomous self-supported climbing robot for inspection applications," proc. Int. Conf. Intelligent Automonous Vehicles, Madrid, Spain,1998

[11]Fukuda,T. and Hosokai, H.(1992a), "A study on an autonomous pipeline maintenance robot(3rd Report, Structure and Control Mark Ⅲ and Obstacle Sensing)", JSME International Journal Series C, Vol. 53, No.492 ,pp.1788-94

[12]Fukuda,T. and Hosokai, H.(1992b), "A study on an autonomous pipeline maintenance robot(4rd Report, Joint Control and its Trajectory Generation for Mark Ⅱ)", JSME International Journal Series C, Vol. 53, No.495 ,pp.2325-30

[13] Dong Yuhua, Gao Huilin, Zhou Jing'en, Feng Yaorong, "Evaluation of gas release rate through holes in pipelines," Journal of Loss Prevention in the Process Industries, 15(2002), pp.423-428.

[14] Xingsong Wang, Fengyu Xu, Conceptual Design and Initial Experiments on Cable Inspection Robotic System, IEEE Int. Conf. on Mechatronics and Automation, Harbin, China, Aug. 6-8, 2007